

Sensing Anomalies like Humans: A Hominine Framework to Detect Abnormal Events from Unlabeled Videos

Siqi Wang^{1*}, Guang Yu^{1*}, Zhiping Cai¹, En Zhu¹, Xinwang Liu¹, Jianping Yin², Chengzhang Zhu¹

¹National University of Defense Technology, ²Dongguan University of Technology
{wangsiqi10c, yuguangnudu}@gmail.com, {zpcai, enzhu, xinwangliu}@nudt.edu.cn
jpyin@dgut.edu.cn, kevin.zhu.china@gmail.com

Abstract

Video anomaly detection (VAD) has constantly been a vital topic in video analysis. As anomalies are often rare, it is typically addressed under a *semi-supervised* setup, which requires a training set with pure normal videos. To avoid exhausted manual labeling, we are inspired by how humans sense anomalies and propose a *hominine* framework that enables both *unsupervised* and *end-to-end* VAD. The framework is based on two key observations: **1)** Human perception is usually local, i.e. focusing on local foreground and its context when sensing anomalies. Thus, we propose to impose *locality-awareness* by localizing foreground with generic knowledge, and a region localization strategy is designed to exploit local context. **2)** Frequently-occurred events will mould humans' definition of normality, which motivates us to devise a *surrogate training* paradigm. It trains a deep neural network (DNN) to learn a surrogate task with unlabeled videos, and frequently-occurred events will play a dominant role in "moulding" the DNN. In this way, a training loss gap will automatically manifest rarely-seen novel events as anomalies. For implementation, we explore various surrogate tasks as well as both classic and emerging DNN models. Extensive evaluations on commonly-used VAD benchmarks justify the framework's applicability to different surrogate tasks or DNN models, and demonstrate its astonishing effectiveness: It not only outperforms existing unsupervised solutions by a wide margin (8% to 10% AUROC gain), but also achieves comparable or even superior performance to state-of-the-art semi-supervised counterparts.

1 Introduction

Video anomaly detection (VAD) (Ramachandra et al., 2020), which aims to detect abnormal events (i.e. anomalies) that deviate from frequently-seen normal routine in surveillance videos, has attracted considerable attention from both academia and industry, owing to its huge potential value to various tasks like automatic video interpretation and emergency management. However, three features of anomalies have rendered VAD a highly challenging problem: **1) Rarity.** Anomalies typically occur at a much lower probability than normal events. **2) Novelty.** Anomalies are usually significantly different from normal events, and they are often unpredictable. **3) Ambiguity.** "Anomaly" is a relative concept without fixed semantics, and its definition often relies on the context. Due to the above three features, it is often hard and less meaningful to collect data of anomalies, which makes the supervised binary classification not directly applicable. Thus, most existing VAD methods follow a *semi-supervised* setup (see Fig. 1(a)), which requires a labeled training set that contains only normal video events. With the training set, a normality model is built, while events that divert from the normality model are viewed as anomalies.

* Authors contribute equally.

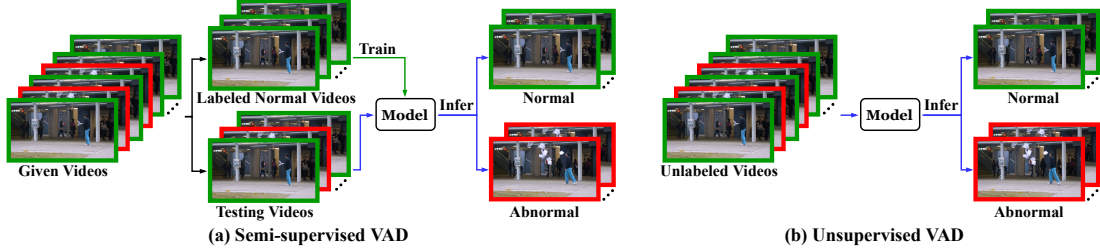


Figure 1: Comparison of different VAD setups.

Although the semi-supervised paradigm enables one to perform VAD without handling the thorny issue of collecting anomaly data, it still has two key limitations: First, building such a training set of normal videos also requires human efforts, and the process can be time-consuming and labor-intensive in itself; Second, since normal events could be innumerable and may evolve with time, the training set may lead to inaccurate description of normal events. More importantly, it should be noted that humans are able to sense anomalies without being specifically taught what normality is. Therefore, recent literature in VAD has witnessed a growing interest in the *unsupervised* setup (see Fig. 1(b)), the goal of which is to discriminate anomalies directly from a bunch of unlabeled videos. Despite that numerous efforts have been made recently (reviewed in Sec. 2), unsupervised VAD still suffers from some important drawbacks: **1) Existing unsupervised solutions are unable to perform end-to-end VAD.** Due to the absence of supervision, most unsupervised VAD methods require hand-crafted feature descriptors, which are scene-dependent and suffer from poor transferability among different scenes. A latest work (Pang et al., 2020) for the first time realizes end-to-end anomaly scoring, but its performance hinges on the initialization step that involves a classic anomaly detection (AD) model (e.g. isolation forest (Liu et al., 2008)). **2) Although VAD is a task originated from humans' subjective cognition, existing unsupervised VAD methods barely take such biological motivations into account.** For example, all existing unsupervised solutions are unexceptionally based on a per-frame basis, but humans tend to identify a local part of the scene as abnormal. Meanwhile, most existing methods are essentially based on detecting drastic local changes, but changes are not equivalent to anomalies for human cognition. **3) The performance of existing unsupervised VAD solutions is still evidently inferior to their semi-supervised counterparts.** Besides, their performance is often reported on relatively simple datasets, while their applicability and effectiveness on a modern dataset like ShanghaiTech (Liu et al., 2018a) are not known.

Our Contributions. Motivated by those gaps above, this paper presents a *hominine* framework that can achieve highly effective VAD in a both *unsupervised* and *end-to-end* manner. Our contributions are three-fold: **1)** Since the human's perception to the scene is local, we propose to impose *locality-awareness* on our unsupervised VAD framework: We leverage generic knowledge to localize each video foreground, and devise a region localization strategy to facilitate the exploitation of local context. **2)** Inspired by the observation that humans tend to naturally define frequently-occurred events in surroundings as normal, we propose *surrogate training* as a new unsupervised VAD paradigm: Given unlabeled video data, we train a deep neural network (DNN) to learn a certain surrogate task. Frequently-occurred events in videos tend to dominate the training, and such dominance enables us to define normality automatically and discriminate novel rarely-seen events as anomalies by a training loss gap. **3)** We explore various surrogate tasks and different DNN models for implementation. By experiments, we not only demonstrate the flexibility of our framework by verifying its effectiveness with those surrogate tasks and DNN models, but also point out the potential way to further enhance VAD performance. On commonly-used VAD benchmarks, our hominine VAD framework achieves a consistent and significant performance improvement against existing unsupervised VAD methods, and its performance is even on par with state-of-the-art semi-supervised solutions.

2 Related Works

Semi-supervised VAD. Semi-supervised VAD has been a thoroughly studied topic. Early classic VAD solutions usually adopt a two-step strategy: They first describe videos by certain hand-crafted descriptors (e.g. trajectory (Piciarelli et al., 2008), dynamic texture (Mahadevan et al., 2010), histogram of optical flow (Cong et al., 2011), 3D gradients (Lu et al., 2013), etc.), and then feeds

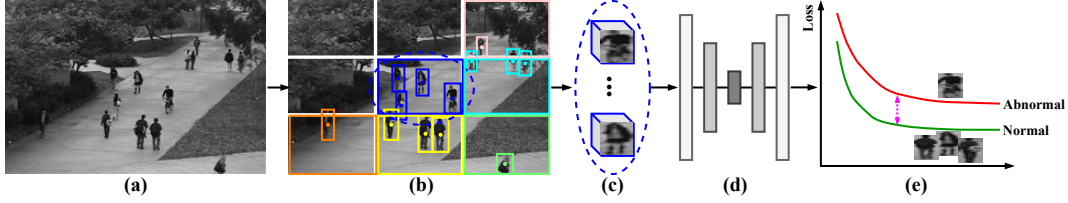


Figure 2: The proposed hominine VAD framework: (a) An input video frame. (b) Imposing locality-awareness by foreground localization and region localization. (c) Building spatio-temporal cubes (STCs). STCs assigned to one local region (e.g. blue region) are analyzed separately. (d) DNN based surrogate training. (e) Detecting anomalies by loss gap between normality and anomalies.

extracted features into a classic AD model (e.g. one-class classifiers (Yin et al., 2008; Wang et al., 2017), probabilistic models (Mahadevan et al., 2010; Cheng et al., 2015), sparse reconstruction models (Cong et al., 2011; Lu et al., 2013; Zhao et al., 2011), nature inspired models (Mehran et al., 2009; Sun et al., 2016), etc.) for training and inference. Due to the success of deep learning, recent years have witnessed an explosive development in DNN based VAD: A straightforward solution is to substitute the feature extraction step by DNN based representation learning (Xu et al., 2015; Tran & Hogg, 2017). Later, recent works usually realize end-to-end VAD by following a frame reconstruction or prediction scheme, and most of them focus on the exploration of more effective DNN architectures, such as convolutional auto-encoder (Hasan et al., 2016), recurrent neural networks (Luo et al., 2017), variational auto-encoder (Yan et al., 2018), U-Net (Liu et al., 2018a), predictive coding network (Ye et al., 2019), etc. A comprehensive review on semi-supervised VAD is provided in (Ramachandra et al., 2020).

Unsupervised VAD. Compared with semi-supervised VAD, unsupervised VAD is a newly-emerging but more challenging topic due to the lack of labeled training data. To our best knowledge, only several attempts have been made in the literature: Del et al. (Del Giorgio et al., 2016) pioneer the exploration by detecting changes in videos as anomalies. Specifically, they describe each video frame by hand-crafted descriptors, and then train a simple classifier to differentiate two temporally consecutive set of features. Afterwards, a good classification indicates a drastic change, while shuffling is used to make the classification order-independent; Tudor et al. (Tudor Ionescu et al., 2017) follow a similar idea to (Del Giorgio et al., 2016), but improve change detection by a more sophisticated unmasking scheme. It iteratively removes the most discriminative feature in the classification, and frames that are still easy to classify after several round of removal are viewed as anomalies; Liu et al. (Liu et al., 2018b) study the connection between unmasking and statistical learning, and further enhance the performance by a history sampling method and a new frame-level motion feature. Unlike above methods that are essentially based on the change detection paradigm, the latest work from Pang et al. (Pang et al., 2020) first obtain the preliminary detection results by leveraging a pre-trained DNN and a classic AD model, and then refine the results by learning to achieve a two-class ordinal regression in a self-trained fashion. As discussed in Sec. 1, existing unsupervised VAD solutions suffer from several drawbacks, which constitute our motivation to propose the new framework in this paper.

3 Hominine VAD Framework

3.1 Locality-awareness

Motivation. An indispensable foundation for our hominine VAD framework is locality-awareness. Our motivation comes from the fact that existing unsupervised VAD methods are unexceptionally carried out on a *per-frame* basis, i.e. VAD is performed based on the entire frame. However, this practice can be problematic: First, humans hardly perceive anomalies on such a large scale. Instead, they usually place more emphasis on the local foreground and its context, which has already been observed in other realms and inspired some widely-used techniques like attention mechanism (Chaudhari et al., 2019). Second, as some recent works (Liu & Ma, 2019; Zhou et al., 2019b) point out, per-frame analysis will distract the model from attending to the foreground part that is more meaningful to VAD, because a large portion of a video frame can be static background. Therefore, we discard per-frame analysis and enable our framework to be aware of locality on both foreground-level and region-level, which are elaborated below.

Foreground Localization. Our first goal is to localize each foreground object in videos for analysis. To this end, we naturally resort to object detection (Liu et al., 2019), which localizes foreground objects by their *appearance*. Due to the lack of training data, we adopt a detector that is pre-trained on a generic large-scale public dataset (e.g. Microsoft COCO (Lin, 2014)). Such generic knowledge enables the pre-trained detector to localize most daily object satisfactorily, and produce a foreground set \mathcal{F}_a based on appearance clue. However, the pre-trained detector lacks the ability to localize novel foreground objects. Motivated by (Yu et al., 2020) that computes temporal gradients to detect active foreground, we introduce optical flow (OF) as a supplementary clue to foreground localization. OF is a frequently-used motion representation that depicts the per-pixel motion between two consecutive frames, and it can be efficiently estimated by a DNN model (e.g. FlowNet v2 (Ilg et al., 2017)) pre-trained on an artificial dataset designed for OF estimation (e.g. FlyingChair dataset (Dosovitskiy et al., 2015)). We choose OF because it is more robust than low-level statistics like gradients used in (Yu et al., 2020). By an algorithm based on contour detection and some simple heuristic rules (detailed in Sec. 1 of supplementary material), we can utilize OF to yield a motion based foreground set \mathcal{F}_m that contains active novel foreground objects. Finally, the final foreground set is obtained by $\mathcal{F} = \mathcal{F}_a \cup \mathcal{F}_m$, while each foreground object $f \in \mathcal{F}$ is marked by a bounding box (see Fig. 2(b)). In this way, we can consider each local foreground object rather than the entire frame for VAD. Besides, the pre-trained detector is only used for localization, and the class information is discarded. For each localized foreground object, D raw patches are extracted from the current and neighboring frames by the location of the object’s bounding box. Finally, those patches are normalized into $H \times W$ patches $\{p_1, \dots, p_D\}$ and stacked into a $H \times W \times D$ spatio-temporal cube (STC) $S = [p_1; \dots; p_D]$. Here, one STC is viewed as the representation of a video event, while it also serves as the basic processing unit in our VAD framework.

Region Localization. Definition of anomaly is tightly connected to local context, since video events at different local regions may have evidently different characteristics (foreground type, depth, speed, size, motion patterns, etc.). Thus, we propose to impose region localization by considering foreground objects in each local region separately, as they can be assumed to share the same local context. To be more specific, a frame is uniformly divided into several local rectangular regions, and each foreground object will be assigned to the region that enjoys the maximum overlap with the object’s bounding box. For simplicity of notion, we equate a foreground object f to its bounding box in later analysis. Since the computation and comparison of overlap among different regions can be troublesome, we introduce the following theorem that can significantly simplify the assignment process:

Theorem 1 *Given an arbitrary n -dimensional hyper-cube f^n in the n -dimensional space ($n \in \mathcal{N}^+$), and the space is uniformly partitioned into infinite equally-sized n -dimensional rectangular regions $\{R_i^n\}_{i=1}^\infty$. Then if f^n ’s geometric center c_f^n and the k -th local region R_k^n satisfy $c_f^n \in R_k^n$, the volume of overlap between f^n and R_k^n , $O(f^n, R_k^n)$, will be guaranteed to attain its maximum, i.e.:*

$$O(f^n, R_k^n) = \sup_i \{O(f^n, R_i^n)\} \quad (1)$$

The proof of Theorem 1 is detailed in Sec. 2 of supplementary material. It suggests that we can assign a foreground object to the region where its bounding box’s geometric center lies in (illustrated in Fig. 2(b)), since such an assignment will guarantee a maximum overlap. This strategy also enables us to yield an unique assignment, although a bounding box may enjoy maximum overlap with multiple regions. Finally, all foreground objects (i.e. STCs) assigned to the same local region are collected to be analyzed separately. Later empirical evaluations show that region localization can significantly improve VAD performance when the video scene undergoes obvious foreground depth variation.

3.2 Surrogate Training

Motivation. Our motivation comes from the fact that existing VAD methods are not consistent with human instinct: For one thing, humans can sense anomalies without explicitly knowing what normality is. They do not require a labeled training set like the semi-supervised setup or an initialization step like (Pang et al., 2020); For another, mainstream unsupervised VAD solutions detect drastic local changes as anomalies (Del Giorno et al., 2016; Tudor Ionescu et al., 2017; Liu et al., 2018b), and the exposition of such changes still relies on hand-crafted descriptors. However, changes are not equivalent to anomalies for human perception, especially considering that there may exist intra-class difference within normal events. Instead, humans’ definition of normality is naturally moulded in their daily life: *Frequently-occurred events are automatically defined as normal events by humans*,

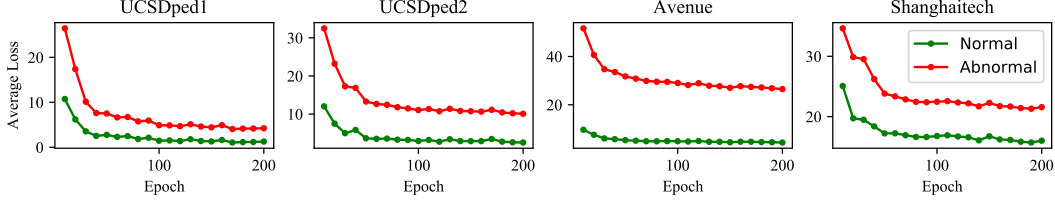


Figure 3: Average training loss of normal and abnormal events on practical video datasets.

while those rarely-seen novel events will be viewed as anomalies. Motivated by such an observation, we propose the *surrogate training* paradigm as a simulation: Given video events extracted from unlabeled videos, we train a DNN to learn a surrogate task (it is called “surrogate” because it is usually not directly relevant to VAD). Similar to how humans’ definition of normality is moulded, intuitively frequently-occurred events will play a dominant role in “moulding” (i.e. training) the DNN. Finally, the anomaly score of a video event can be indicated by how well the DNN fulfills the surrogate task. To illustrate this intuition theoretically, we provide a simple example below.

Theoretical Implication. Consider an batch of data that consists of two evidently different classes, class 1 with N_1 data and class 2 with N_2 data, while all data are normalized into $[-1, 1]$ and $N_1 \gg N_2$. From the perspective of humans, they will naturally view data from class 1 and class 2 as normal and abnormal respectively. For surrogate training, we consider a simple surrogate task that intends to map all data in the batch to a non-zero target t , which can be formulated as a regression problem. To make theoretical analysis possible, we introduce a simple three-layer feed-forward neural network (NN) with L hidden nodes. A single output node with sigmoid activation is used to perform this surrogate task, and we set $0 < t < 1$ to match the output range. To understand how data from two classes “mould” the NN in surrogate training, we consider the NN weights between the hidden and output layer, $\mathbf{w} = (w_1, \dots, w_L)^\top$ (bias is not used), which are directly responsible for regression. The NN can be trained by back-propagation and a mean square error (MSE) loss. With the k_{th} class’s loss in surrogate training denoted by \mathcal{L}_k ($k = 1, 2$), we can view the magnitude of \mathcal{L}_k ’s gradient vector w.r.t \mathbf{w} , $\|\nabla_{\mathbf{w}} \mathcal{L}_k\|$, as a direct indication of how strong the k_{th} class “mould” the NN in surrogate training. By the proof given in Sec. 3 of supplementary material, we have the following theorem:

Theorem 2 When the weight w_i is randomly initialized by an independent uniform distribution on $[-1, 1]$, the expectation of square gradient magnitude w.r.t, \mathbf{w} , $E_{\mathbf{w}}(\|\nabla_{\mathbf{w}} \mathcal{L}_k\|^2)$, is approximated by:

$$E_{\mathbf{w}}(\|\nabla_{\mathbf{w}} \mathcal{L}_k\|^2) \approx \frac{(2t-1)^2 \cdot L}{256} N_k^2, \quad k = 1, 2 \quad (2)$$

Based on the above theorem, it can be derived that $E_{\mathbf{w}}(\|\nabla_{\mathbf{w}} \mathcal{L}_1\|^2)/E_{\mathbf{w}}(\|\nabla_{\mathbf{w}} \mathcal{L}_2\|^2) \approx N_1^2/N_2^2$ since both t and L are constant. As $N_1 \gg N_2$, it indicates that the normal class (class 1) will exert a significantly larger influence than abnormal class (class 2) in surrogate training. Motivated by such a theoretical implication, we conduct some empirical validations on practical video datasets as well (see Fig. 3): Despite that a different surrogate task (presented in Sec. 4.1) is used to implement our framework, empirical results also suggest a constant existence of a training loss gap between normal and abnormal events in surrogate training. Consequently, such results have unveiled the possibility to discriminate anomalies by the loss gap between normality and anomalies in surrogate training.

Remarks. In some sense, the proposed surrogate training is similar to self-supervised learning (Jing & Tian, 2020), which also creates additional supervision that is not directly relevant to the final downstream task. However, we also need to point out the essential difference between self-supervised learning and surrogate training: The goal of self-supervised learning is to learn data representations, and the learned representations will then be used to perform the downstream task. By contrast, representation learning does not play a center role in surrogate training. Instead, it intends to manifest the training loss gap between anomalies and normality, which can be used for VAD in an end-to-end manner.

4 Implementations

4.1 Surrogate Tasks

As we mentioned in Sec.3.1, we consider the STC of each foreground object, $S = [p_1; \dots; p_D]$, as the basic processing unit. Analogous to the frame reconstruction and frame prediction scheme that are prevalent in semi-supervised VAD, we devise two categories of surrogate tasks: *STC recovery* and *STC completion*, which are tailored for unsupervised VAD by taking locality of foreground into account. As to STC recovery, we first impose a certain transformation on a STC S to obtain a transformed STC \tilde{S} , and then train a DNN to recover the original STC. Meanwhile, we also introduce another DNN to recover the optical flow of each patch $\{m_1, \dots, m_D\}$ from \tilde{S} . This is because motion is another important attribute of videos, and optical flow has already been computed in foreground localization. We explore three frequently-used transformations: **1)** Identity transformation $\tilde{S} = [p_1; \dots; p_D]$. **2)** Reverse transformation $\tilde{S} = [p_D; \dots; p_1]$. **3)** Random shuffling transformation $\tilde{S} = [p_{r_1}; \dots; p_{r_D}]$, where $\{r_1, \dots, r_D\}$ is a random permutation of index $\{1, \dots, D\}$. Thus, three transformations correspond to three different surrogate tasks. As to STC completion, we erase the last patch p_D and obtain an incomplete STC $\hat{S} = [p_1; \dots; p_{D-1}]$. Two DNNs are then trained to infer the missing patch p_D and its optical flow m_D respectively. As both STC recovery and STC completion are generative, they can be trained by MSE loss function. It should be noted that one can certainly explore a more sophisticated surrogate task other than four basic tasks above.

4.2 DNN Models

We explore both classic and emerging DNN models to carry out a surrogate task. As for the classic DNN model, we choose convolutional auto-encoder (CAE), which is one of the most popular DNN models in VAD and unsupervised deep learning. Specifically, CAE first maps a STC to a low-dimensional embedding by a fully-convolutional multi-layer encoder \mathcal{E} , and then the desired outputs are expected to be decoded from the embedding by a fully-convolutional decoder \mathcal{D} . For example, for STC recovery based surrogate tasks, CAE is supposed to realize the following goal:

$$S = \mathcal{D}(\mathcal{E}(\tilde{S})) \quad (3)$$

Apart from classic CAE, we also explore an emerging DNN model, vision transformer (ViT) (Dosovitskiy et al., 2020), for surrogate training. To illustrate how ViT is tailored for surrogate training, we take STC recovery as an instance: Given the j -th patch $p_j \in \mathbb{R}^{H \times W}$ in the input STC \tilde{S} (the channel number is ignored here), we first flatten it into a 1-d vector $v_j \in \mathbb{R}^{(H \cdot W)}$, and map it to an embedding $v'_j \in \mathbb{R}^d$ as follows:

$$v'_j = \text{Lin}(v_j) + e_j \quad (4)$$

where $\text{Lin}(\cdot)$ denotes a learnable linear mapping, while $e_j \in \mathbb{R}^d$ is a learnable positional embedding. The sequence of embedding, $[v'_1, \dots, v'_D]$, is then fed into Y consecutive blocks that are identical. Each block comprises of three modules: Multi-head self-attention module (*MSA*), layer normalization module (*LN*) and feed forward (*FF*) module. As inputs and outputs of each block share the same size, ViT computes the outputs of y -th ($y \in \{1, \dots, Y\}$) block, $Z^y = [z_1^y, \dots, z_D^y]$, as follows:

$$\begin{aligned} \hat{Z}^y &= \text{MSA}(\text{LN}(Z^{y-1})) + Z^{y-1} \\ Z^y &= \text{FF}(\text{LN}(\hat{Z}^y)) + \hat{Z}^y \end{aligned} \quad (5)$$

Eventually, we map each item $z_j^Y \in \mathbb{R}^d$ in outputs Z^Y to the original dimension $\tilde{z}_j^Y \in \mathbb{R}^{(H \cdot W)}$ with another trainable linear layer, and reshape it to a 2-d patch $\tilde{p}_j \in \mathbb{R}^{H \times W}$ to obtain the generated STC $\tilde{S} = [\tilde{p}_1; \dots; \tilde{p}_D]$. For STC completion, the input of ViT is an incomplete STC with $(D - 1)$ patches $\hat{S} = [p_1; \dots; p_{D-1}]$, and it expects ViT to output a single patch for completion. Thus, we compute the output of ViT by an average of $(D - 1)$ output items: $z^Y = \frac{1}{D-1} \sum_{j=1}^{D-1} z_j^Y$. To our best knowledge, this is also the first time that ViT is applied for VAD. In fact, the point to explore different DNN models is not limited to validate the applicability of the proposed framework. More importantly, our empirical evaluations show that the ensemble of DNN models that are trained for one surrogate task proves to be a simple but effective way to further enhance VAD performance.

Table 1: Performance comparison with state-of-the-art unsupervised and semi-supervised VAD solutions. AUC-F and AUC-P denote frame-level and pixel-level AUROC respectively.

Type	Method	UCSDped1		UCSDped2		Avenue	ShanghaiTech
		AUC-F	AUC-P	AUC-F	AUC-P	AUC-F	AUC-F
Semi-supervised	CAE (Hasan et al., 2016)	81.0%	-	90.0%	-	70.2%	-
	SRNN (Luo et al., 2017)	-	-	92.2%	-	81.7%	68.0%
	Recounting (Hinami et al., 2017)	-	-	92.2%	89.1%	89.8%	-
	Frame-Prediction (Liu et al., 2018a)	83.1%	-	95.4%	-	85.1%	72.8%
	Att-prediction (Zhou et al., 2019b)	83.9%	-	96.0%	-	86.0%	-
	PDE-AE (Abati et al., 2019)	-	-	95.4%	-	-	72.5%
	Mem-AE (Gong et al., 2019)	-	-	94.1%	-	83.3%	71.2%
	AM-Corr (Nguyen & Meunier, 2019)	-	-	96.2%	-	86.9%	-
	AnomalyNet (Zhou et al., 2019a)	83.5%	45.2%	94.9%	52.8%	86.1%	-
	GEPC (Markovitz et al., 2020)	-	-	-	-	-	76.1%
	OGNet (Zaheer et al., 2020)	-	-	98.1%	-	-	-
	Clustering-AE (Chang et al., 2020)	-	-	96.5%	-	86.0%	73.3%
	SIGNet (Fang et al., 2020)	86.0%	51.6%	96.2%	48.4%	86.8%	-
	Multispace (Zhang et al., 2020)	-	-	95.4%	-	86.8%	73.6%
	MPED-RNN (Morais et al., 2019)	-	-	-	-	86.3%	73.4%
	Mem-Guided (Park et al., 2020)	-	-	97.0%	-	88.5%	70.5%
	AnoPCN (Ye et al., 2019)	-	-	96.8%	-	86.2%	73.6%
	Scene-Aware (Sun et al., 2020)	-	-	-	-	89.6%	74.7%
	VEC (Yu et al., 2020)	-	-	97.3%	-	89.6%	74.8%
	SRNN-AE (Luo et al., 2021)	-	-	92.2%	-	83.5%	69.6%
	Online (Doshi & Yilmaz, 2021)	-	-	97.2%	-	86.4%	70.9%
	AMMC (Cai et al., 2021)	-	-	96.6%	-	86.6%	73.7%
Unsupervised	Discriminative (DeI Giorno et al., 2016)	59.6%	-	63.0%	-	78.3%	-
	Unmasking (Tudor Ionescu et al., 2017)	68.4%	52.4%	82.2%	-	80.6%	-
	MC2ST (Liu et al., 2018b)	71.8%	-	87.5%	-	84.4%	-
	STDOR (Pang et al., 2020)	71.7%	-	83.2%	-	-	-
	Hominine (ours)	81.7%	61.9%	97.2%	90.4%	92.5%	75.1%

4.3 Anomaly Scoring

Since our hominine VAD framework utilizes the training loss gap to discriminate anomalies, we can conveniently leverage the loss of a video event during surrogate training to realize end-to-end anomaly scoring. As we described in Sec. 4.1, the surrogate tasks devised above all require to perform patch generation and optical flow generation, which correspond to an appearance loss \mathcal{L}_a and motion loss \mathcal{L}_m respectively. Thus, for a STC S , we can define the following anomaly score:

$$\mathcal{A}(S) = \omega_a \cdot \frac{\mathcal{L}_a(S) - \bar{\mathcal{L}}_a}{\sigma_a} + \omega_m \cdot \frac{\mathcal{L}_m(S) - \bar{\mathcal{L}}_m}{\sigma_m} \quad (6)$$

where $\bar{\mathcal{L}}_a$ and σ_a denote the mean and standard deviation for all STCs' appearance loss, and $\bar{\mathcal{L}}_m$ and σ_m are similarly defined. $\bar{\mathcal{L}}_a, \sigma_a, \bar{\mathcal{L}}_m, \sigma_m$ are used to normalize the appearance loss and motion loss into a comparable scale, and they are readily accessible since unsupervised VAD follows a transductive learning paradigm. Our experiments show that a simple anomaly score defined in Eq. (6) has already been able to produce surprisingly good VAD performance. Besides, to further boost performance, we calculate the anomaly score by combining different DNN models: $\mathcal{A}(S) = \mathcal{A}_{ViT}(S) + \mathcal{A}_{CAE}(S)$, where $\mathcal{A}_{ViT}(S)$ and $\mathcal{A}_{CAE}(S)$ correspond to the anomaly score yielded by ViT and CAE model respectively (note that both CAE and ViT are trained to learn the same surrogate task here).

5 Experiments

5.1 Experimental Settings

To evaluate the proposed hominine VAD framework, we conduct experiments on the following publicly available benchmark datasets: UCSDped1/ped2² (Mahadevan et al., 2010), Avenue³ (Lu et al., 2013) and ShanghaiTech⁴ (Liu et al., 2018a), which are also the most frequently-used datasets

²<http://www.svcl.ucsd.edu/projects/anomaly/dataset.htm>

³<http://www.cse.cuhk.edu.hk/leo/jia/projects/detectabnormal/dataset.html>

⁴https://svip-lab.github.io/dataset/campus_dataset.html

Table 2: Ablation Studies for foreground localization (FL) and region localization (RL) using CAE. Note that RL is only applied to UCSDped1 and ShanghaiTech to handle varied foreground depth.

Dataset	UCSDped1			UCSDped2		Avenue		ShanghaiTech		
Config.	w/o Locality	FL	FL+RL	w/o Locality	FL	w/o Locality	FL	w/o Locality	FL	FL+RL
AUC	71.0%	71.3%	81.8%	81.1%	96.7%	87.6%	91.1%	64.2%	72.6%	74.9%

Table 3: Ablation Studies on DNN model ensemble. Note that the anomaly scores yielded by each individual model is not smoothed here to enable raw performance comparison of those models.

Dataset	UCSDped1			UCSDped2			Avenue			ShanghaiTech		
Config.	CAE	ViT	CAE+ViT	CAE	ViT	CAE+ViT	CAE	ViT	CAE+ViT	CAE	ViT	CAE+ViT
AUC	80.5%	78.2%	80.6%	95.2%	95.3%	95.8%	90.7%	91.6%	92.1%	74.0%	74.0%	74.2%

in current VAD research. To perform unsupervised VAD, we follow the setup of previous work (Pang et al., 2020) and merge the original train/test set into one unlabeled video dataset for VAD, while all provided labels are only used for evaluation. To conduct quantitative evaluation, we adopt the standard *frame-level* criteria and *pixel-level* criteria in VAD (Mahadevan et al., 2010): Frame-level criteria consider a video frame that is labeled as abnormal to be correctly detected if any pixel on the frame is identified as abnormal. By contrast, pixel-level criteria are more challenging as the anomaly localization is also required (Mahadevan et al., 2010): One abnormal video frame can only be considered to be correctly detected when more than 40% pixels of anomalies on this frame are correctly identified. With either of two criteria, we can compute Area Under Receiver Operation Characteristic Curve (AUROC) as a quantitative performance measure. Following the common practice in literature, we perform both frame-level and pixel-level evaluation for UCSDped1 and UCSDped2 dataset as they provide fine-grained pixel-level label masks, while only frame-level evaluation is performed on other datasets. We adopt the reverse transformation based surrogate task for the proposed framework by default. The final anomaly scores are obtained by the ensemble of CAE and ViT, which are then smoothed by a sliding window. Region localization is applied to UCSDped1 and ShanghaiTech dataset as they both suffer from evident foreground depth variation (shown in Fig. 2 of supplementary material). As previous works do, running time is not reported as unsupervised VAD is an offline transductive learning problem. Full implementation details are provided in supplementary material.

5.2 Experimental Results

Comparison with State-of-the-art Methods. We compare our hominine VAD framework against 4 existing unsupervised VAD solutions, while we also include 22 state-of-the-art semi-supervised VAD solutions as a reference. As shown by results in Table 1, we can draw the following two observations: **1) Our hominine VAD framework has significantly advanced the performance of unsupervised VAD.** Specifically, our framework leads the best performer among existing unsupervised solutions (MC2ST (Liu et al., 2018b)) by about 8% to 10% AUROC. Meanwhile, it is worth mentioning that our framework is the only solution that achieves both unsupervised and fully end-to-end VAD, which completely avoids introducing hand-crafted descriptors or a separated classic AD model. Besides, we also notice that our framework is the only unsupervised VAD solution that reports fairly satisfactory performance on the recent ShanghaiTech dataset, which is more challenging than other datasets due to its larger scale and diverse scenes. **2) Our unsupervised framework for the first time achieves comparable or even superior VAD performance to semi-supervised solutions.** In particular, our framework outperforms most semi-supervised solutions on three commonly-used datasets for DNN based VAD (UCSDped2, Avenue and ShanghaiTech), and it even achieves 92.5% AUROC on Avenue, which is the best performance ever achieved on this dataset within our knowledge. Although the performance of our framework on UCSDped1 is still highly competitive, it is degraded by the low-resolution gray-scale frames, which undermines the foreground localization. This is also the reason why few recent works report their performance on UCSDped1. Last but not the least, it should be noted that many previous works also take advantage of generic knowledge from pre-trained DNN models, e.g. the unsupervised STDOR (Pang et al., 2020) as well as the semi-supervised Recounting (Hinami et al., 2017), AM-Corr (Nguyen & Meunier, 2019), and Frame-Prediction (Liu et al., 2018a). Nevertheless, our framework still outperforms them by a notable margin.

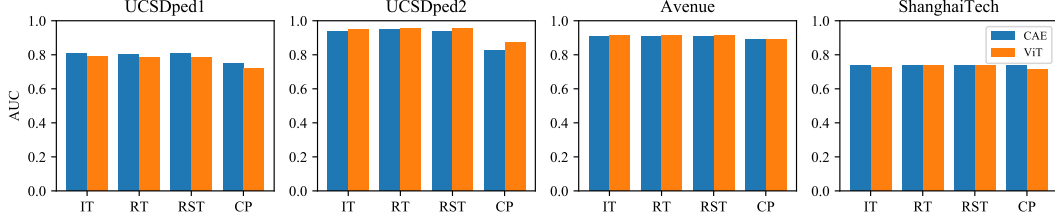


Figure 4: Influence of different surrogate tasks and DNN models.

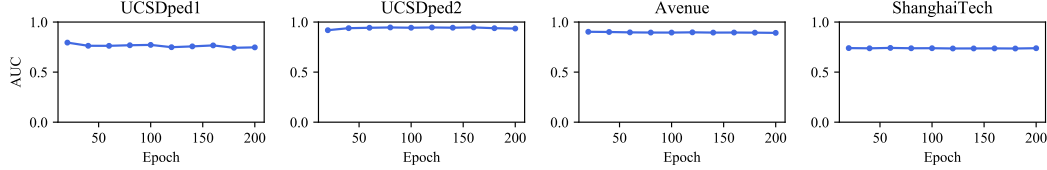


Figure 5: Influence of the training epoch number.

Ablation Studies Ablation studies are conducted to justify the effectiveness of locality-awareness and ensemble, which are displayed in Table 2 and Table 3 respectively. The results lead to three conclusions: **1) Foreground localization plays a critical role in the proposed hominine VAD framework.** Specifically, foreground localization produces a remarkable performance improvement (4.5%-15% AUROC gain) on most datasets when compared to the case where surrogate training is directly applied, which suggests that it is the key to successful surrogate training. On UCSDped1, the improvement is marginal due to the comparatively poor localization caused by low-resolution gray-scale frames. **2) Region localization can significantly improve VAD performance in case where foreground depth varies.** For the dataset with foreground depth variation (UCSDped1 and ShanghaiTech), we can observe a prominent performance improvement up to 10%. However, our experiments show that region localization does not improve performance on other datasets, since their foreground has close depth or gathers in a local region. In fact, the division of local regions for fixed-camera scene can be easily performed by empirical observation on video frames. **3) The ensemble of different DNN models constantly performs better than a single model.** This can be ascribed to the complementary representations learned by different DNN models in surrogate training, which may enable our framework to achieve further performance improvement by combining more DNN models.

Discussion. We discuss the influence of three key factors: **1) Surrogate tasks.** We compare the VAD performance of three STC recovery tasks based on identity transformation (IT), reverse transformation (RT) and random shuffling transformation (RST), as well as a STC completion task (CP). As shown in Table 4, three STC recovery tasks obtain fairly close VAD performance. By contrast, STC completion typically performs worse than three STC recovery tasks, but it still produces better VAD performance than existing unsupervised VAD solutions. Thus, such an observation verifies our framework’s applicability to different surrogate tasks. **2) DNN models.** In general, CAE and ViT produce slightly different VAD performance in each experimental configuration, but none of them possesses consistent advantage against the other. As we discussed above, different DNN models are likely to focus on learning different aspects of video data, which can be complementary and benefit VAD performance. Furthermore, it also suggests that other DNN models can be explored for this framework. **3) Training epoch number.** A natural question is whether the loss gap will gradually vanish as the training epoch number increases. To answer this question, we visualize the VAD performance w.r.t the training epoch number in Fig. 5. Interestingly, VAD performance basically remains stable as the training continues on different benchmark datasets, despite some minor fluctuations. In addition, experiments also suggest that the performance of our framework will rapidly rise to a satisfactory level in a small number of epochs like 10–20. Thus, such favorable features make our framework convenient to train.

6 Conclusion

In this paper, we propose a highly effective hominine VAD framework, which further bridges the gaps between machine-aided VAD and human cognition. By virtue of the novel locality-awareness and surrogate training, our framework can achieve both unsupervised and end-to-end VAD without

involving any hand-crafted features or classic AD model, and it is shown to be applicable to different surrogate tasks and DNN models. Experiments demonstrate our framework’s astonishing effectiveness when compared with both state-of-the-art unsupervised and semi-supervised VAD solutions.

Limitations and Future Directions. Our framework has three major limitations: **1)** Its application is still limited to the fixed-camera scenario. Current foreground localization method will fail in videos with non-stationary background. Therefore, it can be promising to realize foreground localization by an open-world object detector. **2)** Only generative learning is considered as surrogate tasks for our framework in this paper. It will be interesting to explore other learning paradigms like discriminative learning or contrastive learning in the future. **3)** The proposed framework does not actively enlarge the loss gap in surrogate training to refine the VAD results. To this end, we can explore an iterative re-weighting paradigm or an adaptive loss function such as focal loss (Lin et al., 2017).

References

- Abati, D., Porrello, A., Calderara, S., and Cucchiara, R. Latent space autoregression for novelty detection. In *Proceedings of the IEEE Conference on Computer Vision and Pattern Recognition*, pp. 481–490, 2019.
- Cai, R., Zhang, H., Liu, W., Gao, S., and Hao, Z. Appearance-motion memory consistency network for video anomaly detection. 2021.
- Chang, Y., Tu, Z., Xie, W., and Yuan, J. Clustering driven deep autoencoder for video anomaly detection. In *ECCV*, 2020.
- Chaudhari, S., Mithal, V., Polatkan, G., and Ramanath, R. An attentive survey of attention models. *arXiv preprint arXiv:1904.02874*, 2019.
- Cheng, K.-W., Chen, Y.-T., and Fang, W.-H. Video anomaly detection and localization using hierarchical feature representation and gaussian process regression. In *Proceedings of the IEEE Conference on Computer Vision and Pattern Recognition*, pp. 2909–2917, 2015.
- Cong, Y., Yuan, J., and Liu, J. Sparse reconstruction cost for abnormal event detection. In *Proceedings of the 2011 IEEE Conference on Computer Vision and Pattern Recognition*, pp. 3449–3456. IEEE Computer Society, 2011.
- Del Giorno, A., Bagnell, J. A., and Hebert, M. A discriminative framework for anomaly detection in large videos. In *European Conference on Computer Vision*, pp. 334–349. Springer, 2016.
- Doshi, K. and Yilmaz, Y. Online anomaly detection in surveillance videos with asymptotic bound on false alarm rate. *Pattern Recognition*, 114:107865, 2021.
- Dosovitskiy, A., Fischer, P., Ilg, E., Hausser, P., Hazirbas, C., Golkov, V., Van Der Smagt, P., Cremers, D., and Brox, T. FlowNet: Learning optical flow with convolutional networks. In *Proceedings of the IEEE international conference on computer vision*, pp. 2758–2766, 2015.
- Dosovitskiy, A., Beyer, L., Kolesnikov, A., Weissenborn, D., Zhai, X., Unterthiner, T., Dehghani, M., Minderer, M., Heigold, G., Gelly, S., et al. An image is worth 16x16 words: Transformers for image recognition at scale. *arXiv preprint arXiv:2010.11929*, 2020.
- Fang, Z., Liang, J., Zhou, J. T., Xiao, Y., and Yang, F. Anomaly detection with bidirectional consistency in videos. *IEEE transactions on neural networks and learning systems*, PP, 2020.
- Gong, D., Liu, L., Le, V., Saha, B., Mansour, M. R., Venkatesh, S., and Hengel, A. v. d. Memorizing normality to detect anomaly: Memory-augmented deep autoencoder for unsupervised anomaly detection. In *The IEEE International Conference on Computer Vision (ICCV)*, October 2019.
- Hasan, M., Choi, J., Neumann, J., Roy-Chowdhury, A. K., and Davis, L. S. Learning temporal regularity in video sequences. In *Proceedings of the IEEE conference on computer vision and pattern recognition*, pp. 733–742, 2016.
- Hinami, R., Mei, T., and Satoh, S. Joint detection and recounting of abnormal events by learning deep generic knowledge. In *Proceedings of the IEEE International Conference on Computer Vision*, pp. 3619–3627, 2017.

- Ilg, E., Mayer, N., Saikia, T., Keuper, M., Dosovitskiy, A., and Brox, T. FlowNet 2.0: Evolution of optical flow estimation with deep networks. In *Proceedings of the IEEE conference on computer vision and pattern recognition*, pp. 2462–2470, 2017.
- Jing, L. and Tian, Y. Self-supervised visual feature learning with deep neural networks: A survey. *IEEE Transactions on Pattern Analysis and Machine Intelligence*, 2020.
- Lin, T. Y. *Microsoft COCO: Common objects in context*. Springer International Publishing, 2014.
- Lin, T. Y., Goyal, P., Girshick, R., He, K., and Dollar, P. Focal loss for dense object detection. In *IEEE International Conference on Computer Vision (ICCV)*, 2017.
- Liu, F. T., Ting, K. M., and Zhou, Z.-H. Isolation forest. In *2008 Eighth IEEE International Conference on Data Mining*, pp. 413–422. IEEE, 2008.
- Liu, K. and Ma, H. Exploring background-bias for anomaly detection in surveillance videos. In *Proceedings of the 27th ACM International Conference on Multimedia*, pp. 1490–1499, 2019.
- Liu, L., Ouyang, W., Wang, X., Fieguth, P., Chen, J., Liu, X., and Pietikainen, M. Deep learning for generic object detection: A survey. *International Journal of Computer Vision*, pp. 1–58, 2019.
- Liu, W., Luo, W., Lian, D., and Gao, S. Future frame prediction for anomaly detection—a new baseline. In *Proceedings of the IEEE Conference on Computer Vision and Pattern Recognition*, pp. 6536–6545, 2018a.
- Liu, Y., Li, C.-L., and Póczos, B. Classifier two sample test for video anomaly detections. In *BMVC*, pp. 71, 2018b.
- Lu, C., Shi, J., and Jia, J. Abnormal event detection at 150 fps in matlab. In *Proceedings of the IEEE international conference on computer vision*, pp. 2720–2727, 2013.
- Luo, W., Liu, W., and Gao, S. A revisit of sparse coding based anomaly detection in stacked rnn framework. In *Proceedings of the IEEE International Conference on Computer Vision*, pp. 341–349, 2017.
- Luo, W., Liu, W., Lian, D., Tang, J., Duan, L., Peng, X., and Gao, S. Video anomaly detection with sparse coding inspired deep neural networks. *IEEE Transactions on Pattern Analysis and Machine Intelligence*, 43:1070–1084, 2021.
- Mahadevan, V., Li, W., Bhalodia, V., and Vasconcelos, N. Anomaly detection in crowded scenes. In *2010 IEEE Computer Society Conference on Computer Vision and Pattern Recognition*, pp. 1975–1981. IEEE, 2010.
- Markovitz, A., Sharir, G., Friedman, I., Zelnik-Manor, L., and Avidan, S. Graph embedded pose clustering for anomaly detection. *2020 IEEE/CVF Conference on Computer Vision and Pattern Recognition (CVPR)*, pp. 10536–10544, 2020.
- Mehran, R., Oyama, A., and Shah, M. Abnormal crowd behavior detection using social force model. In *2009 IEEE Computer Society Conference on Computer Vision and Pattern Recognition (CVPR 2009), 20-25 June 2009, Miami, Florida, USA, 2009*.
- Morais, R., Le, V., Tran, T., Saha, B., Mansour, M., and Venkatesh, S. Learning regularity in skeleton trajectories for anomaly detection in videos. In *Proceedings of the IEEE Conference on Computer Vision and Pattern Recognition*, pp. 11996–12004, 2019.
- Nguyen, T.-N. and Meunier, J. a. Anomaly detection in video sequence with appearance-motion correspondence. In *Proceedings of the IEEE International Conference on Computer Vision*, pp. 1273–1283, 2019.
- Pang, G., Yan, C., Shen, C., Hengel, A. V. D., and Bai, X. Self-trained deep ordinal regression for end-to-end video anomaly detection. *2020 IEEE/CVF Conference on Computer Vision and Pattern Recognition (CVPR)*, pp. 12170–12179, 2020.

- Park, H., Noh, J., and Ham, B. Learning memory-guided normality for anomaly detection. *2020 IEEE/CVF Conference on Computer Vision and Pattern Recognition (CVPR)*, pp. 14360–14369, 2020.
- Piciarelli, C., Micheloni, C., and Foresti, G. L. Trajectory-based anomalous event detection. *IEEE Transactions on Circuits and Systems for video Technology*, 18(11):1544–1554, 2008.
- Ramachandra, B., Jones, M., and Vatsavai, R. R. A survey of single-scene video anomaly detection. *IEEE Transactions on Pattern Analysis and Machine Intelligence*, 2020.
- Sun, C., Jia, Y., Hu, Y., and Wu, Y. Scene-aware context reasoning for unsupervised abnormal event detection in videos. *Proceedings of the 28th ACM International Conference on Multimedia*, 2020.
- Sun, Q., Liu, H., and Harada, T. Online growing neural gas for anomaly detection in changing surveillance scenes. *Pattern Recognition*, pp. S0031320316302771, 2016.
- Tran, H. T. and Hogg, D. Anomaly detection using a convolutional winner-take-all autoencoder. In *Proceedings of the British Machine Vision Conference 2017*. British Machine Vision Association, 2017.
- Tudor Ionescu, R., Smeureanu, S., Alexe, B., and Popescu, M. Unmasking the abnormal events in video. In *Proceedings of the IEEE International Conference on Computer Vision*, pp. 2895–2903, 2017.
- Wang, S., Zhu, E., Yin, J., and Porikli, F. Video anomaly detection and localization by local motion based joint video representation and oclm. *Neurocomputing*, 277(FEB.14):161–175, 2017.
- Xu, D., Ricci, E., Yan, Y., Song, J., and Sebe, N. Learning deep representations of appearance and motion for anomalous event detection. In *Proceedings of the British Machine Vision Conference*, pp. 8.1–8.8, 2015.
- Yan, S., Smith, J. S., Lu, W., and Zhang, B. Abnormal event detection from videos using a two-stream recurrent variational autoencoder. *IEEE Transactions on Cognitive and Developmental Systems*, 2018.
- Ye, M., Peng, X., Gan, W., Wu, W., and Qiao, Y. Anopc: Video anomaly detection via deep predictive coding network. In *Proceedings of the 27th ACM International Conference on Multimedia*, pp. 1805–1813. ACM, 2019.
- Yin, J., Yang, Q., and Pan, J. J. Sensor-based abnormal human-activity detection. *IEEE Transactions on Knowledge and Data Engineering*, 20(8):1082–1090, 2008.
- Yu, G., Wang, S., Cai, Z., Zhu, E., Xu, C., Yin, J., and Kloft, M. Cloze test helps: Effective video anomaly detection via learning to complete video events. In *Proceedings of the 28th ACM International Conference on Multimedia*, pp. 583–591, 2020.
- Zaheer, M., ha Lee, J., Astrid, M., and Lee, S. Old is gold: Redefining the adversarially learned one-class classifier training paradigm. *2020 IEEE/CVF Conference on Computer Vision and Pattern Recognition (CVPR)*, pp. 14171–14181, 2020.
- Zhang, Y., Nie, X., He, R., Chen, M., and Yin, Y. Normality learning in multispace for video anomaly detection. *IEEE Transactions on Circuits and Systems for Video Technology*, pp. 1–1, 2020.
- Zhao, B., Fei-Fei, L., and Xing, E. P. Online detection of unusual events in videos via dynamic sparse coding. In *CVPR 2011*, pp. 3313–3320. IEEE, 2011.
- Zhou, J. T., Du, J., Zhu, H., Peng, X., Liu, Y., and Goh, R. S. M. Anomalynet: An anomaly detection network for video surveillance. *IEEE Transactions on Information Forensics and Security*, 2019a.
- Zhou, J. T., Zhang, L., Fang, Z., Du, J., Peng, X., and Yang, X. Attention-driven loss for anomaly detection in video surveillance. *IEEE Transactions on Circuits and Systems for Video Technology*, 2019b.